



Friction Coefficient Evolution of Drying Lubricant in the Joints of Beetles by Friction Force Microscopy

Cornelia F. Pichler¹ · Richard Thelen¹ · Thomas van de Kamp^{2,3} · Hendrik Hölscher¹

Received: 25 October 2024 / Accepted: 16 January 2025 / Published online: 4 February 2025
© The Author(s) 2025

Abstract

Recent studies suggest that the joints of beetles and other insects comprise micro-structured surfaces in combination with lubricants. Here, we utilize friction force microscopy (FFM) to analyse the tribological properties of the femoro-tibial leg joints by the example of *Coelorrhina aurata* (metallic green flower beetle) and *Otiorhynchus sulcatus* (black vine weevil). To preserve the original state of the lubricant as well as the microstructures, the FFM measurements were conducted in silicone oil, which satisfies our requirements of transparency, customizable viscosity, absent health risks and lower density compared to the expected density of the lubricant. Microscopic friction was measured on fresh and air-dried samples to stress the change of the lubricant properties over time. Despite the similarity of the two beetle joints, the FFM measurements reveal different frictional properties of the respective lubricants.

Keywords Bio-tribology · Micro-tribology · Friction force microscopy · Atomic force microscopy · Natural lubricants

1 Introduction

Practically, all moving parts in engineered machinery experience friction and wear, resulting in unwanted energy loss and respective damaging of the moving surfaces in contact. These effects are commonly reduced by lubricants [1, 2]. However, most of these are fossil-based and therefore, sustainable alternatives are needed for a so-called green economy [3–5]. In 2017, Holmberg and Erdemir calculated that 20% of the global energy consumption is due to friction alone [6]. They predict that a reduction of global CO₂ emissions of 3,140 MtCO₂, corresponding to savings of 970

000 million Euros, might be possible in the long term by implementing advanced tribological technologies, including green lubricants. Here, a look into living nature might be an inspiration to find suitable solutions [7, 8]. The joints of mammals, for example, utilize water-based lubricants [9–11], which might serve as prototypes for the development of environmentally friendly alternatives. Insects with exoskeletal joints show resemblance to bearings commonly used in mechanical engineering, both in interactions with the environment and geometry, with the most prominent example of the nut-and-screw joint which can be found in weevils [12]. However, due to the comparatively small size of insect joints, their analysis is challenging.

In recent studies, Nadein et al. [11–13] discovered a fluid-like material in beetle joints and identified it as a lubricant. Although its exact functionality is still unknown, we adopt this label in the following. An inspection with the SEM revealed that this lubricant is found in femoro-tibial joints as well as other joints in several insects. The analysis of the lubricant of *Zophobas morio* (darkling beetle) in a tribometer revealed a coefficient of friction (COF) comparable to that of Teflon. The chemical analysis of the lubricant material with Fourier-transform infrared spectroscopy suggests the biological fluid might be protein-based [13]. A subsequent theoretical study of Filippov et al. [16] suggested that the lubricant forms semi-solid cylinders to reduce friction.

✉ Cornelia F. Pichler
cornelia.pichler@partner.kit.edu

✉ Hendrik Hölscher
hendrik.hoelscher@kit.edu

¹ Institute of Microstructure Technology (IMT), Karlsruhe Institute of Technology (KIT), Hermann-von-Helmholtz Platz 1, 76344 Eggenstein-Leopoldshafen, Germany

² Institute for Photon Science and Synchrotron Radiation (IPS), Karlsruhe Institute of Technology (KIT), 76344 Eggenstein-Leopoldshafen, Germany

³ Laboratory for Applications of Synchrotron Radiation (LAS), Karlsruhe Institute of Technology (KIT), P.O. box 3640, 76021 Karlsruhe, Germany

The lubricant is also suspected to influence the wear of the joint [17].

Due to the tiny amounts of lubricant found in beetle joints, its frictional analysis is challenging. Nadein et al. [13], for example, collected the lubricant from 60 femora to get 0.04 mm^3 of material for their analysis. In a subsequent study, Nadein et al. [15] focussed on the friction of the femoro-tibial joint of *Z. morio* and *Pachnoda marginata*. They measured the COF of the tribological system femur/tibia. To target the challenge of tiny amounts of material, friction force microscopy (FFM)—based on atomic force microscopy (AFM)—is the ideal tool as it can measure friction down to the nanometre scale [18, 19] Consequently, we apply FFM/AFM to analyse the friction of beetle's joint surfaces and the lubricants found in the joints of beetles. Since we are interested in the frictional properties of a setting resembling the natural system as closely as possible, the FFM measurements were conducted directly on the frictional area of the joints of the beetles *Coelorrhina aurata* (Scarabaeidae: Cetoniinae, Fig. 1a) and *Otiorhynchus sulcatus* (Curculionidae: Entiminae, Fig. 1b). *C. aurata* enables us to compare our measurements with the results of predecessor studies [13, 15], which studied beetles from the same subfamily (Cetoniinae) of a similar size, with a similar joint morphology. The weevils (Curculionidae), on the other hand, are well-known due to their peculiar coxa-trochanteral

joints, which closely resemble engineered screw-and-nut joints. This fascinating morphological geometry provokes to have a closer look at the frictional properties and inspired to use this family as a research subject. To maintain the comparability between the two beetles as well as previous studies, we focus solely on the femoro-tibial joint. Analysing the change of the frictional properties over time, we observed different properties of the lubricants of the two beetles. The frictional properties of the lubricant of the rose beetle *C. aurata*, change hardly over a drying period of up to eleven months. The frictional coefficient of the lubricant found in the weevil *O. sulcatus*, however, increased almost tenfold in just six months.

2 Experimental

2.1 Beetle Species

The two examined species of beetles are the green metallic flower beetle *Coelorrhina aurata* (Scarabaeidae: Cetoniinae; Fig. 1a) and the black vine weevil *Otiorhynchus sulcatus* (Curculionidae: Entiminae; Fig. 1b). Both were kept in terrarium boxes. Typical live spans of two months (*C. aurata*) and two to ten months (*O. sulcatus*) were reached, respectively. Since SEM and AFM measurements of the joints of

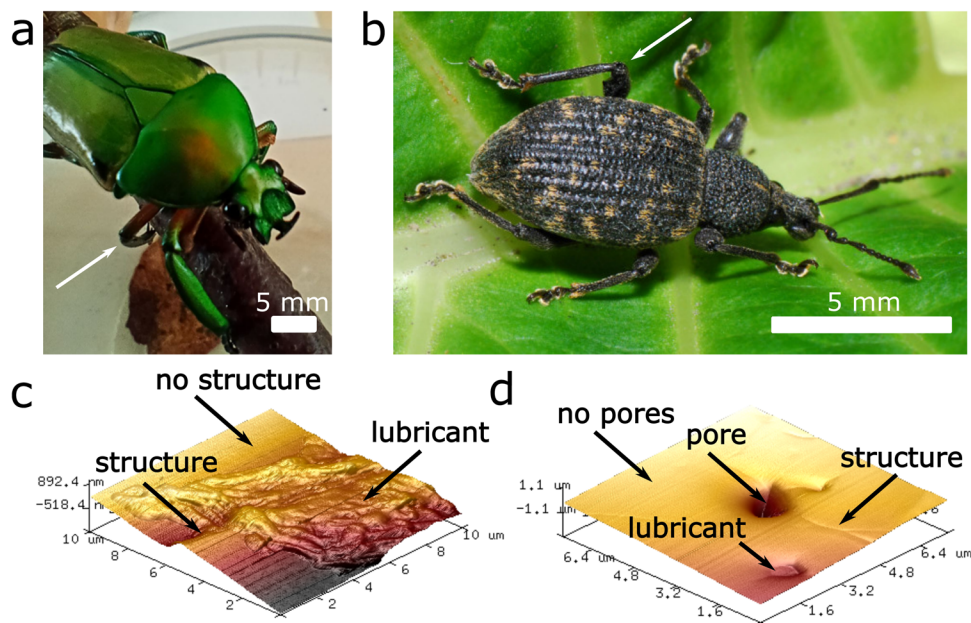


Fig. 1 The two beetle species analysed in this study. **a** The green metallic flower beetle (or rose beetle), *Coelorrhina aurata*. **b** The black vine weevil, *Otiorhynchus sulcatus*. The white arrows point exemplary to the analysed femoro-tibial joints. **c** AFM topography image of one position on the femur of the femoro-tibial joint of *C. aurata* measured in silicone oil in contact mode (scan size: $10 \mu\text{m} \times 10 \mu\text{m}$). The regions of interest for the COF analysis were

identified as labelled above. (1) no structure (2) structure (3) lubricant. **d** AFM topographical image of a position on the femur of the femoro-tibial joint of *O. sulcatus* measured in silicone oil in contact mode (scan size: $7.5 \mu\text{m} \times 7.5 \mu\text{m}$). The regions of interest for the COF analysis were identified as imaged above: (1) no pores (2) pore (3) structure (4) lubricant

living beetles are not possible, we examined the joints after their natural death. For that, the particular beetle's legs were dissected, and the femoro-tibial joints (marked in Fig. 1 with white arrows) were opened manually with a scalpel for further preparation. For the samples, labelled "fresh" in the following, the process was carried out directly after the beetles' death to preserve their natural state as good as possible. This process was carried out as fast as possible (less than an hour). To prove that this preparation approach resulted in "fresh" samples compared to dried ones, we conducted the same procedure with air-dried samples, where the respective dead beetle was stored in a closed sample box for time spans of two weeks, six months and 11 months before preparation (see Tab. S1). The respective storing times are given in the following for each measurement. For the measurements, all successfully opened joints were used, since the examinations with the used measurement devices showed no indication for any tribological difference between the three pairs of legs each beetle possesses.

Four living adults of the rose beetle *C. aurata* were purchased from thePetFactory (Germany, www.thepetfactory.de). These beetles originate from Africa, but they are often found in the homes of beetle enthusiasts, since they display eye-catching colours, and they are easy to breed. Feeding them with beetle jelly (www.thepetfactory.de, Germany), we kept and bred them for one generation on an optimized substrate (combination of Beetlefix 1 & Beetlefix 2, www.thepetfactory.de, Germany). This procedure resulted in five further adults, which were examined, too.

14 living imagines of the weevil *O. sulcatus* were collected in August 2022 and June 2023 in Karlsruhe, Germany. These weevils were fed with fresh leaves of *Tradescantia zebrina* (silver-inch plant) and *Tilia parvifolia* (small-leaved

linden). We observed that this diet feeds the beetles well, after offering them multiple different readily available plants.

2.2 Scanning Electron Microscopy

To get an overview of the general structure, we imaged the femoro-tibial joints of the beetles by scanning electron microscopy (SEM) with a Supra 60 VP (Zeiss, Germany). The samples were fixed on the SEM stub with carbon stickers and sputtered with a layer of ≈ 7 nm of silver. The images were recorded at 3 keV and typical working distances between 3 and 10 mm.

2.3 Friction Force Microscopy

The friction measurements were conducted with a Dimension Icon AFM (Bruker Cooperation, USA). To avoid further drying of the lubricant, all samples were measured in a Petri dish filled with silicone oil (50 cSt, Reeley, Germany). We choose this liquid for the following reasons. To keep the lubricant pinned to the surface without risking a lift-off and floating of the beetle's lubricant, a fluid lighter than water was needed. Furthermore, its viscosity had to be low enough to scan the cantilever undisturbed through the liquid. Silicone oil is a clear choice because of its availability, ease-of-use, transparency, customization, and absent health risks (it is used in hydraulics of kid toys). A fluid probe holder (High Efficiency Direct Drive Tapping Mode Fluid Probe Holder Version 2, Bruker Cooperation, USA) was used to allow such measurements. Figure 2 displays the schematic experimental setup of the AFM holder in the petri dish.

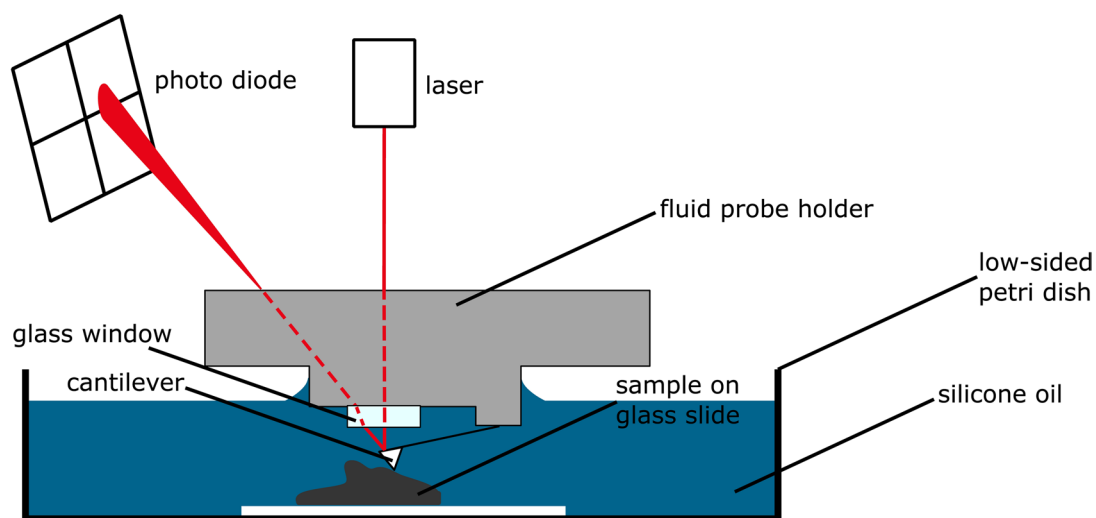


Fig. 2 Schematic of the applied FFM/AFM setup (not to scale). Since the samples had to be immersed in silicone oil to prevent drying, they were placed in a low-sided petri dish and a fluid probe holder was used to mount the cantilever

Commercial rectangular silicon cantilevers were used for all measurements (Budget Sensors, All-in-One-AI, nominal frequency and spring constant are 150 kHz and 7.4 N/m, respectively). After mounting them into the fluid holder, the “Deflection Error Sensitivity” calibration on a flat sapphire surface, and thermal tune, the cantilever and holder were immersed in a low-sided petri dish together with the sample in silicone oil. The calibration procedure of Anderson et al. [20], which links the cantilever torsion of the cantilever (measured in Volt by the AFM) to the equivalent friction force (in Newton), was performed in silicone oil on a sapphire half sphere with a diameter of 0.4 mm.

The recorded data sets were corrected for an instrument-specific tilt, which changed with the cantilever and laser alignment, by subtracting the average of a friction measurement carried out on a flat glass surface. This procedure and the calibration were repeated between sample changes to account for any drift.

The respective measurements of each beetle were recorded with the same cantilever for fresh and air-dried samples to ensure comparability. The cantilevers were calibrated with the sapphire half sphere before measurements of the beetle’s joints. During this first scanning, the tip apex flattened already. After that procedure, we did not observe noticeable wear in contact with the sample, i.e., no changes in topography were detected. Negative friction data and implied negative COF, as a result from insensitivity of the measurement device and obstructing cuticle of the beetle samples, were excluded from the data analysis (twelve scans secluded from a total of 89 recorded scans).

2.4 Frictional Analysis

The contacting areas of the beetle joints feature flat and micro-structured areas, as well as areas with residues of lubricant. Scanning the respective joints with the AFM, the obtained scans comprise all these three areas. Therefore, we had to inspect the surface topography of all data sets to assign them as “flat”, “micro-structured”, or “lubricant”. After that, we were able to extract the respective frictional values from friction loops (Fig. S1).

The goal of this study is to analyse the lubricating properties of the biological fluid, which can be found in the joints of beetles. This can be done by obtaining the COF via FFM and comparing it between beetles, dryness states, and unlubricated and structured chitin. As a frictional property, which can be easily compared, we choose the classical coefficient of friction μ . On the nano- and microscale, it is best defined through the well-known linear friction law [21]

$$F_{fric} = F_0 + \mu F_{load}, \quad (1)$$

where F_{fric} is the measured frictional (lateral) force, F_0 considers possible offsets, and F_{load} is the applied loading force.

To obtain the respective COF, the friction of the beetle surface needs to be recorded at different loads. The friction measurements were therefore conducted from the lowest possible deflection set point in fluid of 1 V, corresponding to about 500 nN, increasing the set point by 1 V steps (with a maximum of 6 V to avoid the risk of cantilever destruction) until the lubricant dislodged and was not visible in the scans anymore. For all COF, data with at least three different increasing deflection set points was analysed. The scans with 512×512 data points, respectively, were analysed visually, consulting both topography and deflection error data to distinguish between the different features of the topography. The respective features were defined as rectangular regions of interest and the frictional data (subtracting retrace from trace of the friction loops and bisect) for each position on the joint of the beetle was averaged, calibrated, plotted versus the loading force, and numerically fitted to Eq. (1). All the resulting COF μ (slopes of the numerical fit) have been averaged for the different features and plotted as bar plots (see the schematic in Figure S2). The error bars, which can be found in Figs. 5b and 6b result from the averaged standard errors of the slopes of the linear fits, weighed by the number of data points. This results in a more accurate picture of the system. The error bars of the averaged frictional data over the loading force in Figs. 5a and 6a are the standard deviation of the frictional data derived from the friction loops. A detailed list of the number of scans, which were used for each feature, is given in Table S1.

3 Results and Discussion

The SEM measurements of fresh and air-dried samples suggested that the lubricant being extruded from pores located on the contact surfaces between the two parts of the joint of the two examined species might differ. While the lubricant of *C. aurata* did not undergo an observable change in the different states of air-drying, the lubricant of *O. sulcatus* showed a considerable change and finally vanishes over time. We, therefore, concluded that the lubricant evaporates almost completely within 48 h and applied the intricate method of recording the friction measurements in silicone oil. These observations have been made on a single beetle, dissecting it on day 0, 1, 2, 4, 8, and 16 after its death, to prevent changes between beetles. The AFM opens many options to measure the tiny amounts of lubricant that have to be handled in this study. To further deepen this lubricant change, the friction measurements of fresh and air-dried samples were compared.

Due to the challenging geometrical properties of the joints of the beetles, the femoro-tibial joint was chosen as

our main research object. Pores extruding lubricant were also found in the coxa and other regions of the femur.

3.1 SEM of the Beetle's Joints

Figure 3a shows SEM images of the tibia of the femoro-tibial joint of *C. aurata*. The zoom on the right shows the pores hidden in the tibia cavity with extruding lubricant. Due to the interlocking movement of the two friction pairs tibia and femur, some lubricant should be transferred naturally to the femur counterpart opposite of the pores in the tibia cavity. By examining the femurs (Fig. 3b), traces of a viscous fluid are visible, which leads us to the assumption, that these traces, which are marked in the magnified image in Fig. 3b with arrows, are lubricant traces. The latter area can be measured with the AFM, due to its flat nature; therefore, we focussed on it during our study. The lubricant of this beetle is also noticeable on the air-dried samples, with no discernible difference.

Figure 4a shows the femur of the researched femoro-tibial joint of *O. sulcatus*. The highlighted crescent area on the joint is the main friction area, where the pores extruding the lubricant are located. Figure 4b shows a collection of those pores in a fresh sample with extruding lubricant, while in

Fig. 4c, the lubricant does not appear in the air-dried samples. The femur part of the femoro-tibial joint presents us with the unique possibility to measure the pores extruding the lubricant directly with the AFM. The crescent friction area hosting the pores is mostly flat and is quite accessible for the AFM.

3.2 FFM of the Femoro-Tibial Joint

The COF of the lubricant of *C. aurata* for three different dryness states (fresh, 2 weeks, 11 months) only changed inside the error bars over time. The higher COF for the structured surface and flat surface over time can be explained by the cracking of the air-dried cuticula.

For *O. sulcatus*, the dried lubricant can be found in tiny amounts in the pores. The air-dried sample was examined 6 months after the beetle's death. For the fresh samples, the lubricant can be found flowing between the pores and covering the pores. The difference between dried and fresh lubricant is quite significant, with the COF of the dried lubricant being 10 times higher than the one from the fresh. The fresh flat area has a COF comparable to the COF of the fresh lubricant, which could lead to the assumption of the lubricant being evenly distributed over the whole friction area.

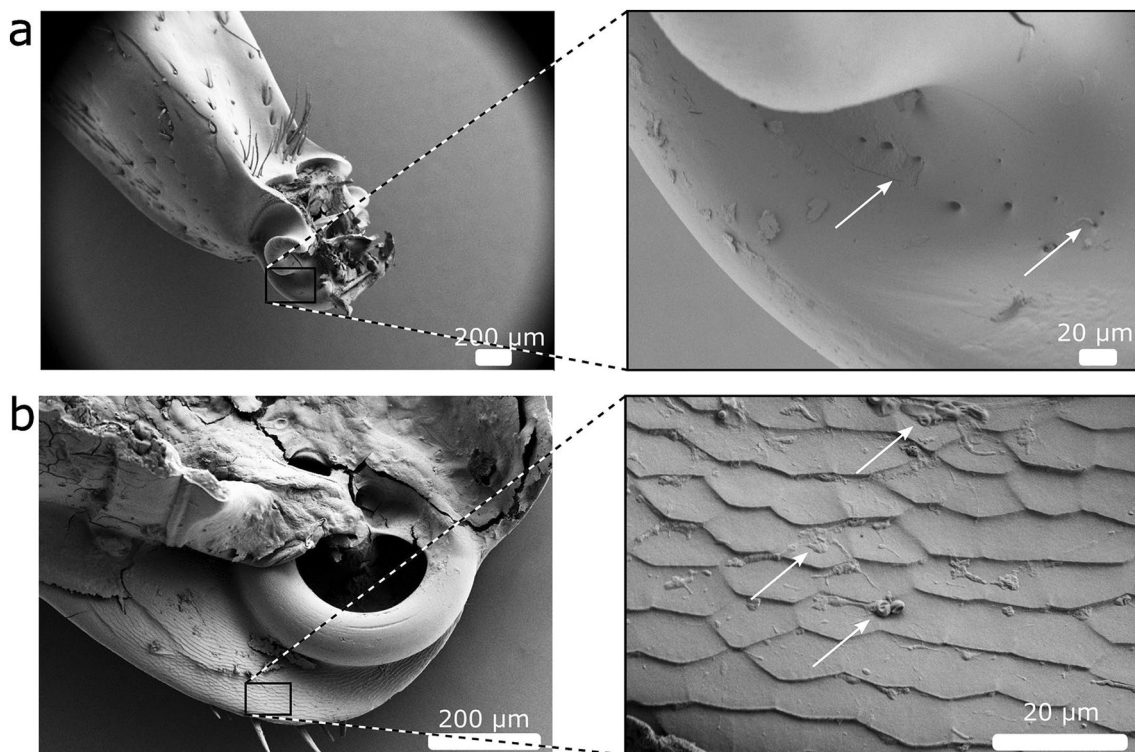


Fig. 3 **a** A SEM image of the tibia of the femoro-tibial joint of *C. aurata*. The joint was dissected shortly after the death of the beetle. Arrows point to lubricant extruding from the pores in the cavity of the tibia part of the femoro-tibial joint. **b** The femur of the femoro-

tibial joint of *C. aurata*, which is the counterpart to the tibia and better accessible with the AFM. The white arrows point to residues of the lubricant

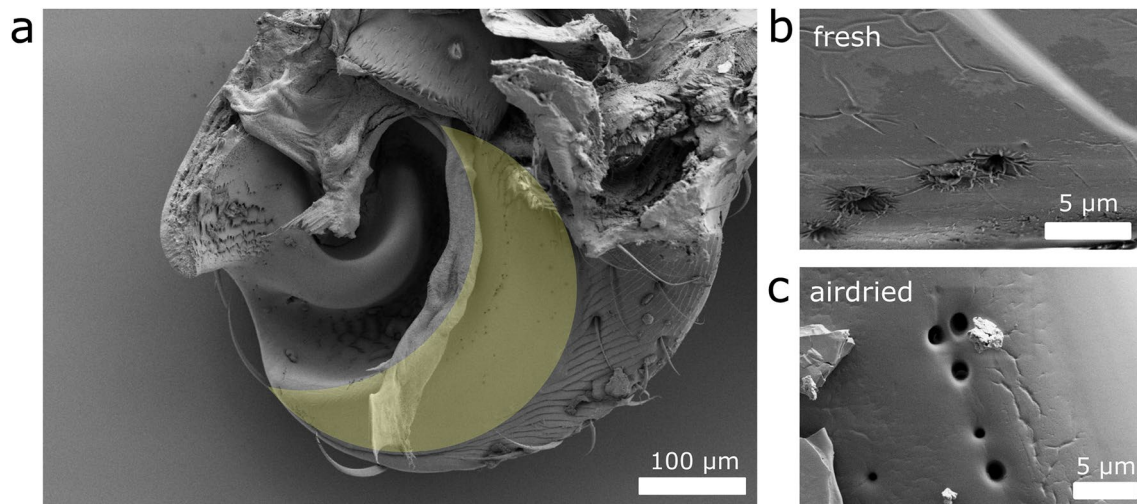


Fig. 4 **a** A SEM image of the femur part of the femoro-tibial joint of *O. sulcatus* dissected after its death. The highlighted crescent surface area is the region of interest, where most of the pores—extruding lubricant—are located. **b** A SEM image of the fresh pores with extruding lubricant and **c** pores in the air-dried state (air-dried for a

month) on the femur part of the femoro-tibial joint of *O. sulcatus*. Pores were also found in the coxa and other regions of the femur. Due to the geometrical constraints of the AFM, the femur pores on the crescent region of the joint were analysed in our study

Figure 1c shows one of the AFM measurements with the different features visible and labelled. Figure 5a shows the calibrated friction force plotted versus the loading force for the different features in a single position of the fresh femur. For this plot, the COF for the single position were extracted. For the COF of the different features of all positions, the separate COF were averaged. The resulting COF for fresh and air-dried samples, with two different drying periods of 2 weeks and 11 months of *C. aurata* are summarized in the bar plot in Fig. 5b.

The femur of the femoro-tibial joint has been examined with the AFM of both fresh and air-dried samples. Since the lubricant showed no visible difference for fresh and air-dried samples under the SEM, the change of the lubricant over a longer time was of interest. The first set of bars average all the recorded AFM images, which includes structures, lubricant etc. and showed a COF of 0.26 ± 0.15 for the sample 11 months old, 0.15 ± 0.06 for the sample two weeks old, and 0.22 ± 0.16 for the fresh sample. The respective COFs show no notable difference between the samples, which means that the distributions of the features are comparable. The sapphire halfsphere, which has been scanned in-between measurements, has comparable COF of 0.09 ± 0.03 , 0.10 ± 0.05 and 0.10 ± 0.04 , respectively.

Having a closer look at the different defining features of the joints of *C. aurata*, we still did not observe a significant change of the COF over time. The flat surface without structures shows comparable COF and as expected the lowest overall of 0.08 ± 0.03 , 0.17 ± 0.06 , 0.09 ± 0.04 , respectively. The researched area of the femur is covered with a shingle-like microstructure, which shows COF of 0.12 ± 0.04

for the oldest sample, 0.24 ± 0.11 for the 2 weeks air-dried sample and 0.24 ± 0.07 for the fresh sample. The microstructure is still an object of ongoing research to explain its function. The lubricant itself undergoes very little change over time, with slightly decreasing COF within the error bars. The COFs for the air-dried samples are 0.34 ± 0.11 and 0.37 ± 0.32 , respectively, and 0.41 ± 0.12 for the fresh lubricants. We, therefore, conclude, that the air-drying of the samples leads to no change in the COF of the joint.

Figure 6 has been constructed in the same way as Fig. 5 to stress the differences between the two beetles. Additional to the features in Fig. 5, the pores, which can be found on the femur of *O. sulcatus* and are accessible with the AFM are included. Figure 1d shows the topography of one scan with the AFM of one position on the fresh femur of *O. sulcatus*. Figure 6a shows the calibrated friction force plotted versus the loading force for the different features in a single position of the fresh femur. The resulting averaged COF for fresh and air-dried samples (6 months) of *O. sulcatus* are summarized in the bar plot in Fig. 6b.

The femur of the femoro-tibial joint has been examined with the AFM of both fresh and air-dried samples. The first bar set includes all AFM measurements, which includes pores, lubricant etc. and the COF for air-dried and fresh samples are quite similar with 0.13 ± 0.04 and 0.16 ± 0.11 , respectively, hinting at a comparable distribution of the features for the different drying states. The sapphire halfsphere, which has been scanned in-between measurements, has a comparable value of 0.15 ± 0.01 and 0.15 ± 0.03 for air-dried and fresh measurements as one would expect for the same cantilever.

Coelorrhina aurata

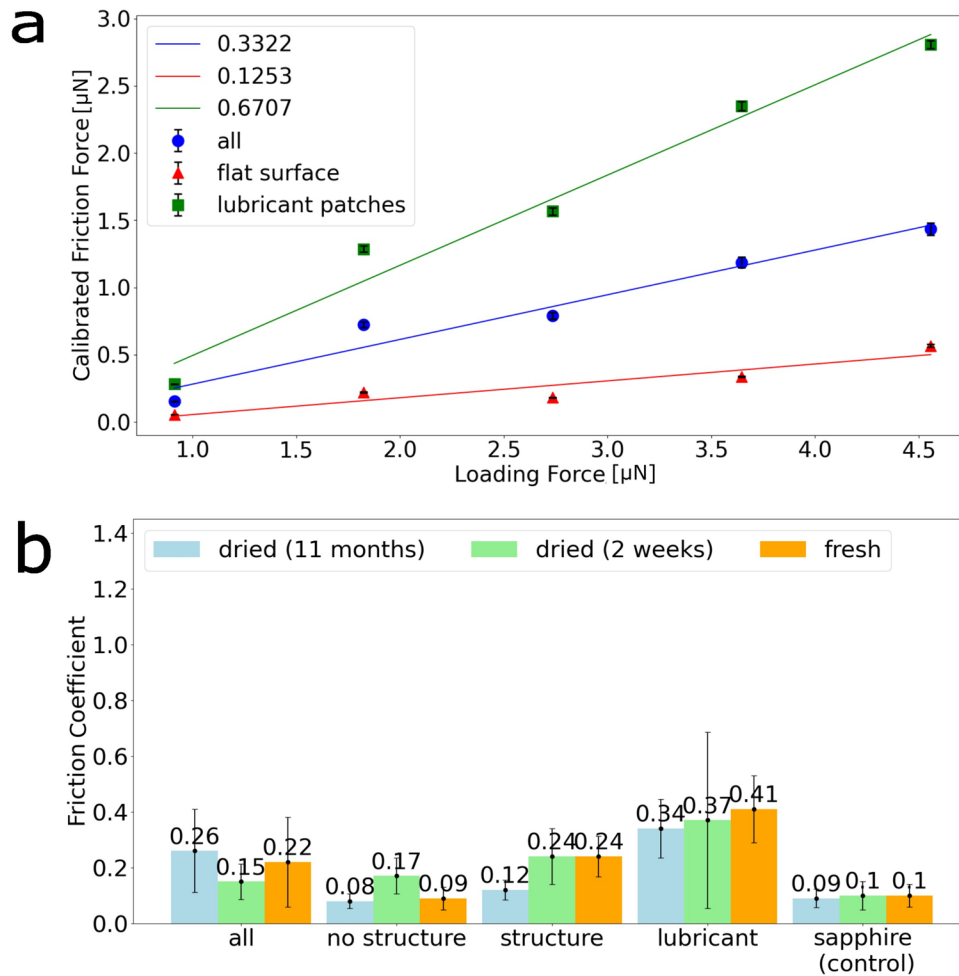


Fig. 5 **a** Exemplary plot of friction force versus loading force of a single position of a fresh sample of the beetle *C. aurata*. Here, the error bars are smaller than the symbol size. **b** Bar plot comparing the COF for dried and fresh samples obtained by averaging several measurements as shown in b). After dissecting a dead beetle *C. aurata*, the samples of the femur part of the joint between the femur and tibia were either directly immersed in silicone oil to prevent the lubricant from evaporating and keep the system as close to the living conditions as possible or air-dried in a closed container for either 2 weeks or 11 months and immersed in silicone oil directly before the meas-

urements. The friction scans were performed with increasing deflection setpoint until the lubricant was no longer visible on the scans and therefore dislodged. The friction scans were firstly analysed including all regions and measurement points, titled in the bar plot as “all”. During the further process, the different interesting areas—namely flat surface (“no structure”), structure and lubricant—were extracted from the scans and analysed. During the calibration procedure, a sapphire halfsphere was scanned and the COF of these measurements are included in this bar plot to highlight the comparability between the scans

The four-bar sets on the left were isolated for their property in all the measurements. Four discernible properties can be differentiated. The pores are the most common features. They have COF within limits of each other, the air-dried with 0.34 ± 0.14 and the fresh pores with 0.30 ± 0.14 . The slightly higher COF for the air-dried sample can be explained by the fact, that the air-dried pores were sometimes filled with dried lubricant with a very high COF, which was not possible to be excluded from the analysis. Around the pores, especially for the air-dried samples, cracking in the cuticula can be observed,

the COF of these structures can be around 0.18 ± 0.08 for the air-dried samples and 0.20 ± 0.21 for the fresh samples, where less cracking is visible, and therefore the error is quite high, due to the reduced amount of data used in this COF. The flat area around the pores is titled “no pores” in the bar chart and has COF of 0.11 ± 0.04 for the air-dried sample, which is counteracted by the cracking of the cuticula and 0.12 ± 0.09 for the fresh sample. The COF of the fresh flat area is strikingly alike to the COF of the fresh lubricant with 0.13 ± 0.09 , which could be construed as the lubricant covering the flat area

Otiorhynchus sulcatus

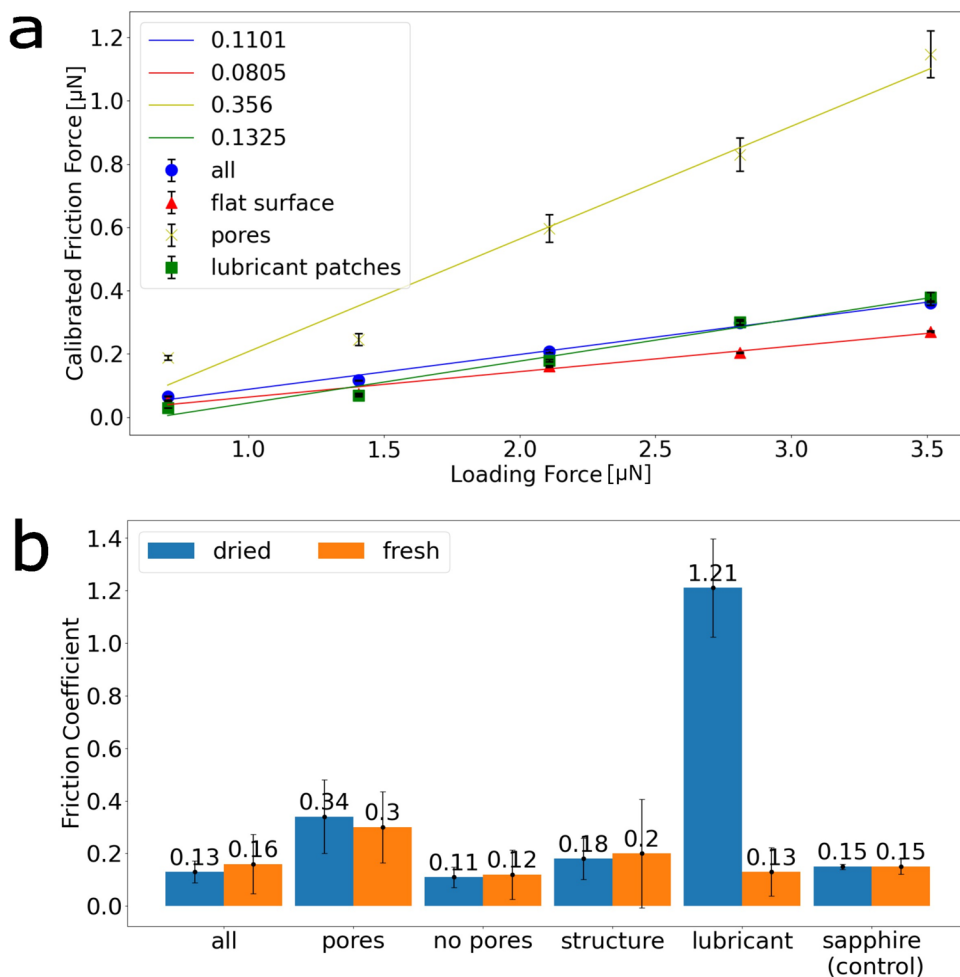


Fig. 6 **a** Calibrated friction force plotted versus the loading force of the different regions of interest of a single position of a fresh sample of *O. sulcatus*. **b** Bar plot comparing the COF for dried and fresh samples. After dissecting a dead beetle *O. sulcatus*, the samples of the femur part of the joint between the femur and tibia were either directly immersed in silicone oil to prevent the lubricant from evaporating and keep the system as close to the living conditions as possible or air-dried in a closed container for 6 months and immersed in silicone oil directly before the measurements. The friction scans were performed at increasing deflection setpoints until the lubricant was no longer visible on the scans and therefore dislodged. The friction

scans were firstly analysed considering all regions and measurement points, which are titled in the bar plot as “all”. During the further process, the different interesting areas—namely flat surface (“no pores”), pores, structure, and lubricant—were extracted from the scans and analysed. For the calibration, a sapphire half sphere was scanned, and the COF of these measurements is included in this bar plot to highlight the comparability between the scans. The lubricant is increasing in adhesion and friction over time. For the fresh sample, the flat surface (no pores) and the lubricant are comparable, which leads us to the assumption, that the surface was covered with a thin layer of lubricant

around the pores, invisible to the AFM measurements. The COF of the dried lubricant is around 10 times higher with 1.21 ± 0.19 .

The significant increase in the COF of the dried lubricant reinforces the results of the SEM that the lubricant of *O. sulcatus* undergoes a change arising from the evaporation during the air-drying process after the beetles’ death.

4 Conclusion

This work researches the lubricants, which can be found in the joints of beetles. The two respective beetles, *Coelorrhina aurata* and *Otiorhynchus sulcatus*, have different kind of lubricants as can be seen in both the SEM analysis

as well as the AFM friction measurements. In the SEM visual analysis of fresh and air-dried samples sputtered with a silver layer of approximately 7 nm – to both aid the SEM imaging and slow down the evaporation process of the lubricant – it can be observed that the lubricant of *Coelorrhina aurata* experiences no changes during the process of air-drying. On the other hand, the lubricant, which can be found in the joints of *Otiorhynchus sulcatus*, visibly disappears during the process of air-drying. This hypothesis is supported by the FFM measurements.

The measurements were conducted in silicone oil to preserve the natural state of the joints and lubricant. The resulting data of the FFM measurements of fresh samples were compared to air-dried samples recorded with the same cantilever and the same setup to enable optimal comparison. For the lubricant of *Coelorrhina aurata*, no significant change in the coefficient of friction was recorded over the time of up to 11 months; while the coefficient of friction of the lubricant of *Otiorhynchus sulcatus* increased by almost a tenfold over the time of just 6 months.

As mentioned in the introduction already, the lubricants of insect joints might be water-based – or at least easily biodegradable – which is a tremendous advantage compared to most fossil-based lubricants. For future experiments, it will be of utmost importance to learn more about the chemistry of the beetle's lubricants, which is a puzzling task due to the small amount of material found in the joints.

Our results evidence that peculiar differences between the lubricants of the beetles exist, *i.e.*, there is not one unique lubricant in beetle joints. Our study compares only two (arbitrary) beetle species. It is expected, however, that approximately 1.5 million, 5.5 million, and 7 million species of beetles, insects, and terrestrial arthropods exist [22]. We, therefore, speculate that many unknown exiting discoveries of tribological interest are waiting to be made in the joints of arthropods.

Acknowledgements We thank Luisa Maren Borgmann for collecting the beetles of the species *Otiorhynchus sulcatus*.

Author Contributions C.F.P., Th.v.K., and H.H. designed the study. C.F.P. conducted the experiments with the support of R.T. and analysed the data. C.F.P. and H.H. wrote the main manuscript text. C.F.P. prepared the figures. All authors reviewed the manuscript.

Funding Open Access funding enabled and organized by Projekt DEAL.

Data Availability Original data sets are available on reasonable request from corresponding author.

Declarations

Competing interests The authors declare no competing interests.

Open Access This article is licensed under a Creative Commons Attribution 4.0 International License, which permits use, sharing, adaptation, distribution and reproduction in any medium or format, as long as you give appropriate credit to the original author(s) and the source, provide a link to the Creative Commons licence, and indicate if changes were made. The images or other third party material in this article are included in the article's Creative Commons licence, unless indicated otherwise in a credit line to the material. If material is not included in the article's Creative Commons licence and your intended use is not permitted by statutory regulation or exceeds the permitted use, you will need to obtain permission directly from the copyright holder. To view a copy of this licence, visit <http://creativecommons.org/licenses/by/4.0/>.

References

- Mate, C.M., Carpick, R.W.: Tribology on the small scale. Oxford University Press, Oxford, UK (2019)
- Khonsari, M.M., Booser, E.R.: Applied Tribology: Bearing Design and Lubrication. John Wiley & Sons (2017)
- Vazquez-Duhalt, R.: Environmental impact of used motor oil. *Sci. Total. Environ.* **79**, 1–23 (1989). [https://doi.org/10.1016/0048-9697\(89\)90049-1](https://doi.org/10.1016/0048-9697(89)90049-1)
- Aluyor, E.O., Ori-jesu, M.: Biodegradation of mineral oils—a review. *Afr. J. Biotechnol.* **8**, 915–920 (2009)
- Tamada, I.S., Lopes, P.R.M., Montagnolli, R.N., Bidoia, E.D.: Biodegradation and toxicological evaluation of lubricant oils. *Braz. Arch. Biol. Technol.* **55**, 951–956 (2012). <https://doi.org/10.1590/S1516-89132012000600020>
- Holmberg, K., Erdemir, A.: Influence of tribology on global energy consumption, costs and emissions. *Friction*. **5**, 263–284 (2017). <https://doi.org/10.1007/s40544-017-0183-5>
- Scherge, M., Gorb, S.S.: Biological Micro- and Nanotribology - Nature's Solutions. Springer (2001)
- Nachtigall, W.: Bionik - Grundlagen und Beispiele für Ingenieure und Naturwissenschaftler. Springer (2002)
- Jin, Z., Dowson, D.: Bio-friction. *Friction*. **1**, 100–113 (2013). <https://doi.org/10.1007/s40544-013-0004-4>
- An, H., Liu, Y., Yi, J., Xie, H., Li, C., Wang, X., Chai, W.: Research progress of cartilage lubrication and biomimetic cartilage lubrication materials. *Front. Bioeng. Biotechnol.* **10**, 1012653 (2022). <https://doi.org/10.3389/fbioe.2022.1012653>
- Dowson, D.: Bio-tribology. *Faraday Discuss.* **156**, 9–30 (2012). <https://doi.org/10.1039/c2fd20103h>
- van de Kamp, T., Vagovic, P., Baumbach, T., Riedel, A.: A Biological screw in a beetle's leg. *Science* **333**, 52–52 (2011). <https://doi.org/10.1126/science.1204245>
- Nadein, K., Kovalev, A., Thogersen, J., Weidner, T., Gorb, S.: Insects use lubricants to minimize friction and wear in leg joints. *Proc. R. Soc. B* **288**, 20211065 (2021). <https://doi.org/10.1098/rspb.2021.1065>
- Nadein, K., Gorb, S.: Lubrication in the joints of insects (*Arthropoda: Insecta*). *J. Zool.* **316**, 24–39 (2021). <https://doi.org/10.1111/jzo.12922>
- Nadein, K., Kovalev, A., Gorb, S.N.: Tribological properties of the beetle leg joints. *Friction*. (2024). <https://doi.org/10.1007/s40544-024-0933-0>
- Filippov, A.E., Nadein, K., Gorb, S.N., Kovalev, A.: Bio-bearings: numerical model of the solid lubricant in the leg joints of insects. *Trib. Lett.* **72**, 11 (2024). <https://doi.org/10.1007/s11249-023-01815-3>
- Nadein, K., Gorb, S.N.: Abrasive wear in the leg joints of insects. *Adv. Mater. Interfaces* **11**, 2300743 (2024). <https://doi.org/10.1002/admi.202300743>

18. Meyer, E., Bennewitz, R., Hug, H.J.: Scanning probe microscopy - the lab on a tip. Springer, Berlin, Heidelberg (2017)
19. Bhushan, B.: Nanotribology and nanomechanics - an introduction. Springer, Berlin, Heidelberg (2017)
20. Anderson, E.V., Chakraborty, S., Esformes, T., Eggiman, D., Degraf, C., Stevens, K.M., Liu, D., Burnham, N.A.: Shape-independent lateral force calibration. *ACS Appl. Mater. Interfaces* **3**, 3256–3260 (2011). <https://doi.org/10.1021/am200770r>
21. Schirmeisen, A., Jansen, L., Hölscher, H., Fuchs, H.: Temperature dependence of point contact friction on silicon. *Appl. Phys. Lett.* **88**, 123108 (2006). <https://doi.org/10.1063/1.2187575>
22. Stork, N.E.: How many species of insects and other terrestrial arthropods are there on earth? *Annu. Rev. Entomol.* **63**, 31–45 (2018). <https://doi.org/10.1146/annurev-ento-020117-043348>

Publisher's Note Springer Nature remains neutral with regard to jurisdictional claims in published maps and institutional affiliations.